Acta Cryst. (1996). D52, 521–528

Structure of a Kunitz-Type Chymotrypsin Inhibitor from Winged Bean Seeds at 2.95 Å Resolution

JIBAN K. DATTAGUPTA,[a]* ALOKA PODDER,[a] CHANDANA CHAKRABARTI,[a] UDAYADITYA SEN,[a] SAMIR K. DUTTA[b] AND MANORANJAN SINGH[b]

[a]*Crystallography and Molecular Biology Division, Saha Institute of Nuclear Physics, 1/AF Bidhan Nagar, Calcutta 700 064, India, and* [b]*Biochemical Engineering Division, Indian Institute of Chemical Biology, Jadavpur, Calcutta 700 032, India*

(*Received 25 July 1995; accepted 3 January 1996*)

Abstract

The crystal structure of an α-chymotrypsin inhibitor ($P6_122$; $a = 61.4$, $c = 210.9$ Å) isolated from winged bean (*Psophocarpus tetragonolobus*) seeds has been determined at 2.95 Å resolution by the molecular-replacement method using the 2.6 Å coordinates of *Erythrina* trypsin inhibitor (ETI) as the starting model (57% sequence homology). This protease inhibitor, WCI, belongs to the Kunitz (STI) family and is a single polypeptide chain with 183 amino-acid residues having a molecular weight of 20 244 Da. Structure refinement with *RESTRAIN* and *X-PLOR* has led to a crystallographic R factor of 19.1% for 3469 observed reflections ($I > 2\sigma$) in the resolution range 8–2.95 Å. A total of 56 water molecules have been incorporated in the refined model containing 181 amino-acid residues. In the refined structure the deviations of bond lengths and bond angles from ideal values are 0.015 Å and 2.2°, respectively. The inhibitor molecule is spherical and consists of 12 antiparallel β-strands with connecting loops arranged in a characteristic folding (a six-stranded β-barrel and a six-stranded lid on one hollow end of the barrel) common to other homologous serine protease inhibitors in the Kunitz (STI) family as well as to some non-homologous proteins like interleukin-1α and interleukin-1β. In the structure the conformation of the protruding reactive-site loop is stabilized through hydrogen bonds mainly formed by the side chain of Asn14, which intrudes inside the cavity of the reactive-site loop, with the side-chain and main-chain atoms of some residues in the loop region. A pseudo threefold axis exists parallel to the barrel axis of the structure. Each of the three subdomains comprises of four β-strands with connecting loops.

1. Introduction

Protease inhibitors are ubiquitous in nature and following the crystallization and characterization of the soybean trypsin inhibitor (STI) by Kunitz in 1947 (Kunitz, 1947*a*,*b*), many protein inhibitors of proteases have been isolated from diverse sources (Laskowski & Sealock, 1971; Ryan, 1973). They are generally grouped into three main families: (i) Kunitz family (ii) Bowman–Birk family and (iii) Kazal family (Laskowski & Kato, 1980). Among the plant sources, leguminous seeds are usually found to be rich in both the Kunitz and the Bowman–Birk types of serine protease inhibitors, some of which have been extensively studied (Richardson, 1977). Their physiological role is yet to be established. However, the elegant studies of Ryan (1990) have provided compelling reasons to implicate them in 'plant-defense' functions against infesting insects as they can act as strong antifeedants. In addition to the antifeedant role, the participation of these inhibitors in the regulation of cellular protein turnover is another interesting possibility since soybean trypsin inhibitor and winged bean chymotrypsin inhibitor are major components of proteosome complexes isolated from developing soybean and winged bean seeds, respectively (Usha & Singh, 1995). Three-dimensional structure determination of a few of these inhibitors as well as of a fewer number of inhibitor–protease complexes by X-ray crystallography (Bode & Huber, 1992) have led to the elucidation of a common mechanism of action of protease inhibitors and a general understanding of the specific protein–protein interactions involving the inhibitors and their cognate proteases at the molecular level. Based on these studies, a reactive-site loop on the surface of the inhibitor molecules has been identified as the structural motif which interacts with the enzyme at its active site, to yield a more or less stable enzyme–inhibitor complex, thus blocking the active site of the enzyme.

The protease inhibitors of winged bean (*Psophocarpus tetragonolobus*) seeds have been studied by several groups (Kortt, 1980; Shibata, Hara, Ikenaka & Abe, 1986; Roy & Singh, 1986). The winged bean chymotrypsin inhibitor (WCI) was first isolated by affinity chromatography employing immobilized chymotrypsin as the affinity ligand (Kortt, 1980). Later, other more conventional column chromatography techniques have been used to isolate the same as well as other protease

inhibitors (Roy & Singh, 1986; Shibata *et al.*, 1986). Apart from other types of inhibitors, the presence of isoinhibitors in winged bean seeds has been emphasised by the findings of Shibata *et al.* (1986), while the protein isolated by us (inadvertently named as '*Psophocarpin* B_1') has been shown to be identical to the chymotrypsin inhibitor originally isolated by Kortt in 1980 (Roy & Singh, 1988). It is now clear that the Kunitz-type chymotrypsin inhibitor studied by Kortt (1980) as well as by Roy & Singh (1986, 1988) is the same as the major isoinhibitor form extensively studied by Shibata *et al.* (1986) and Shibata, Hara & Ikenaka (1988). It is a single-chain polypeptide having 183 amino-acid residues and a molecular mass of 20 244 Da calculated from the primary sequence determined by Shibata *et al.* (1988). It occurs abundantly in the seeds and tubers of winged bean plants.

An unusual stoichiometry of binding has been revealed in the interaction of WCI and chymotrypsin (Kortt, 1980; Shibata *et al.*, 1986). Unlike other Kunitz-type inhibitors which commonly have a 1:1 molar ratio while binding to their target proteases, 1 mol of WCI binds 2 mol of chymotrypsin. Prolonged incubation of WCI with chymotrypsin at pH 4.1 has enabled Shibita *et al.* (1988) to identify Leu65–Ser66 as a scissile bond and a reactive-site loop has been tentatively located around this bond. However, these studies have not revealed a second scissile bond.

The Kunitz (STI) family of inhibitors, of which WCI is a member, is characterized by the presence of two disulfide bridges and a molecular mass of about 20 kDa. Crystal structures of two other members of this family have been reported – both are trypsin inhibitors, one being STI complexed with porcine trypsin (Blow, Janin & Sweet, 1974; Sweet, Wright, Janin, Chothia & Blow, 1974) and the other *Erythrina* trypsin inhibitor (ETI) (Onesti, Brick & Blow, 1991). The structure of another serine protease inhibitor, PKI3 (proteinase K inhibitor) from wheat germ, also belonging to the Kunitz family, has been reported (Zemke, Müller-Fahrnow, Jany, Pal & Saenger, 1991). However, the crystal structure of any chymotrypsin inhibitor in the family has not been reported so far.

2. Materials and methods

2.1. *Isolation of WCI*

WCI was isolated from imbibed winged bean seeds either by the method described by Roy & Singh (1986) or by the affinity chromatography method of Kortt (1980) using immobilized chymotrypsin and trypsin columns. The homogeneity of all preparations were checked by sodium dodecyl sulfate polyacrylamide gel electrophoresis (SDS–PAGE) (Laemmli, 1970) and immunoblot analysis (Towbin, Staehelin & Gordon, 1979) using the rabbit immune serum (Roy & Singh, 1986).

2.2. *Crystals and crystal data*

Elongated single crystals of WCI were obtained by us at pH 8.0 using the vapour-diffusion method (Dattagupta, Podder, Chakrabarti, Dutta & Singh, 1990). The crystals, which grow up to maximum dimensions of $0.7 \times 0.3 \times 0.3$ mm, belong to the hexagonal space group $P6_122$ with cell parameters $a = b = 61.4$ and $c = 210.9$ Å, with one molecule (20 244 Da) in the crystal asymmetric unit and a solvent content of 57%(v/v) (Matthews, 1968). Intensity data up to 2.95 Å resolution were collected on a Siemens–Nicolet multiwire area detector on a GX 20 Marconi Avionics rotating-anode X-ray generator. The raw data were processed by using *XENGEN* (Howard *et al.*, 1987). A total of 3913 unique reflections out of 9549 observations were obtained with a merging R ($R_{\rm merge} = \sum |I - \langle I \rangle| / \sum I$, where I = observed intensity, $\langle I \rangle$ = average intensity obtained from multiple observations of symmetry-related reflections) of 4.6%, which account for ~85% of the expected number of reflections to 2.95 Å resolution.

2.3. *Structure solution by molecular replacement*

The structure of the inhibitor was solved by the molecular-replacement technique using the 2.6 Å resolution coordinates (made available to us by Dr D. M. Blow, Imperial College of Science and Technology, London) of ETI, which has about 57% sequence homology with WCI, as the search model. Some of the residues that differed between ETI and WCI were initially treated as alanine. Normalized structure factors for space group $P1$ were calculated for the resulting molecule positioned in a unit cell of dimensions $64 \times 64 \times 72$ Å by the programs *GENSFC* and *ECALC* of the *CCP*4 suite (Collaborative Computational Project, Number 4, 1994). The cross-rotation functions were calculated between the model and WCI data using *ALMN*, based on the fast-rotation function of Crowther (1972). After several trials, using different Patterson radii and different resolution ranges of data, the highest rotation peak was obtained in a function using radii of 3–27 Å and data-resolution range of 10–4 Å. The highest peak appeared at $\alpha = 57.5$, $\beta = 60$, $\gamma = -127.5°$. Although this rotation peak (2.5 r.m.s. density) was not much higher than the next highest peak (1.7 r.m.s. density), it appeared in almost all the trials. The translation functions corresponding to this peak were then calculated using the T_2 function (Crowther & Blow, 1967) as implemented in the program *TFSGEN* of the *CCP*4 package. Fourier coefficients of the T_2 function were calculated for space groups $P6_122$ and $P6_522$ in the resolution range 10–4 Å. A T-function map was generated using the program *FFT* (Ten-Eyck, 1973)

for both the space groups for half the unit cell along the z axis. A unique solution for the space group $P6_122$ was obtained at $x = 0.744$, $y = 0.295$ and $z = 0.037$ with a peak height 15.4 r.m.s. density compared to the second highest peak of height 7.9 r.m.s. density. No such prominent peak appeared for the space group $P6_522$.

2.4. *Structure refinement*

The initial model yielded an R factor of 47% confirming the plausibility of the molecular replacement solution. Two cycles of rigid-body refinement with the data in the 11–4 Å resolution range using the program *RESTRAIN* (Driessen *et al.*, 1990) reduced the R factor to 45%. After five more cycles of constrained restrained refinement, the R value dropped to 43%. A σ_A-weighted (Read, 1986) $2F_o - F_c$ map was then used to build the WCI sequence into the density employing a Silicon Graphics workstation using the interactive computer program *TOM* (Jones, 1978; Cambillau & Horjales, 1987). The model was further improved by alternating cycles of refinement and model building using $2F_o - F_c$ and $F_o - F_c$ maps. Density for three amino-terminal residues, eight carboxy terminal residues and residues 95–100 and 136–143 was ambiguous and they were not included in the model at this stage. After rebuilding portions of the molecule, making adjustments in the side chains and the main chains as needed, the model was subjected to conjugate-gradient minimization and simulated-annealing refinement using *X-PLOR* (Brünger, 1992). After positional, slow-cooling and regularization steps the R value fell to 25.7% in the resolution range 11–4 Å. The electron-density maps calculated during the course of refinement improved steadily and most of the missing residues could be fitted to the maps. Three N-terminal residues, three near the C terminus (Lys176, Ser177 and Glu178) and residues 95–100, 136, 138, 139 and 143 could now be added to the model leading to an R factor of 22.3% for 11–3 Å resolution data. Water molecules were introduced at this stage by examining the new $2F_o - F_c$ and $F_o - F_c$ maps. Unidentified and distinct electron-density peaks which appeared in these maps were regarded as water molecules if they were within 3.7 Å from a protein donor or acceptor group or from another water molecule. The occupancies of the water molecules were fixed to 1.0 and their isotropic temperature factors were assigned a value of 20 Å^2. Further positional and slow-cooling refinement at 1000 K with the standard slow-cooling and individual B-factor refinement led to an R factor of 20.9%. All missing residues except 179 and 180 could now be incorporated in the model. After one more round of *X-PLOR* refinement, the crystallographic R factor for data between 11 and 3 Å converged to 20.1%. The resolution range was next changed to 8–2.95 Å and refinement in this range yielded better stereochemistry for the model. More water molecules could be located in difference Fourier maps and the final model contains 56 water molecules. Only two amino-acid residues, Thr179 and Ala180 remained unlocated. The final R factor is 19.1% for 3469 observed reflections in the resolution range 8–2.95 Å.

Table 1. *Crystallographic R factor as a function of resolution*

Resolution range (Å)	Observed reflections	% Configuration	R value
8.00–5.34	613	88.71	21.26
5.34–4.47	591	89.14	16.79
4.47–3.98	520	78.79	16.28
3.98–3.66	452	71.18	18.52
3.66–3.42	416	66.88	19.69
3.42–3.23	376	59.22	20.62
3.23–3.08	284	45.22	22.87
3.08–2.95	217	34.89	26.24

3. Results and discussion

3.1. *Quality of the structure*

The electron density for the main chain is continuous except at residues Thr179 and Ala180 near the C terminus. The side chains of Lys108, Lys112, Lys121, His137, Asp138 and Arg152 also have not been included in the model beyond CB. Some representative portions of the $2F_o - F_c$ map calculated using the final model are shown in Fig. 1. The distribution of the crystallographic R factor against resolution range is given in Table 1. In the model the r.m.s. deviations from ideality of bond lengths, bond angles, dihedral angles and improper angles are 0.015 Å, 2.2, 28.1 and 1.9°, respectively.

Fig. 2. shows the distribution of the backbone conformational angles φ and ψ in the form of the Ramachandran plot (Ramakrishnan & Ramachandran, 1965). The side-chain dihedral angles were checked to be satisfactory with *PROCHECK* (Laskowski, MacArthur, Moss & Thornton, 1993).

3.2. *General features*

The protein molecule is approximately spherical with overall dimensions 48 × 46 × 46 Å and its structure is similar to the structures of other legume seed serine proteinase inhibitors, like STI and ETI, from the same Kunitz (STI) family. These molecules share an architecture consisting of 12 antiparallel β-strands connected by long loops. These loops dominate the surface of the molecule. A C^α chain superposition of the three homologous structures (STI, ETI and WCI) of the family is given in Fig. 3. The external loops including the reactive-site region show deviations, though the core region is conserved. The r.m.s. deviations for the β-strands of WCI from those of ETI and STI are smaller (0.36 Å for 55 C^α positions and 0.46 Å for 53 C^α

positions, respectively) than those for the loop regions (0.73 Å for 84 C^{α} positions and 0.80 Å for 71 C^{α} positions, respectively) (Subbarao & Haneef, 1991). The relative orientation of the reactive-site loop of WCI is in between those in STI and ETI. The folding of the molecule is such that the N-terminus comes close to the reactive-site loop (Fig. 4*a*) whereas in the ETI structure both the C and N termini are near the reactive-site loop. Six of the 12 β-strands form a β-barrel and the other six form a cover closing one hollow end of the barrel (Fig. 4*a*). The β-barrel formed by parallel or antiparallel β-strands usually with a hydrophobic core inside the barrel, is a popular motif found in proteins (Chothia & Janin, 1982; Farber & Petsko, 1990). The number of β-strands varies from five to 13 in barrels (Richardson, 1981). All the members of the Kunitz (STI) family are characterized by the presence of a six-stranded antiparallel β-barrel. A schematic representation of the secondary structure of WCI is shown in Fig. 4(*b*). Another interesting feature observed is the presence of a pseudo threefold symmetry axis parallel to the barrel axis and passing through the centre of the molecule. The three subdomains related by the pseudo threefold axis are also indicated in Fig. 4(*b*). Each subdomain is formed by four β-strands: the first strand from the barrel, second and third ones from the barrel-cover and the fourth one again from the barrel. This characteristic folding of the structure follows the pattern described by McLachlan (1979) and is observed in STI, ETI, and also in interleukin-1β (Priestle, Schär & Grütter, 1988, 1989; Finzel *et al.*, 1989), interleukin-1α (Graves *et al.*, 1990) and PKI3 (Zemke *et al.*, 1991). The short antiparallel six-stranded β-barrel in WCI has a hydrophobic core made up of the side chains of Tyr18, Leu20, Ile58, Ile60, Val75, Leu77, Phe79, Phe117, Phe119, Leu132, Tyr130, Leu170 and Leu172 (Fig. 5). The polar end of the two tyrosine residues project outwards, the hydrophobic parts being well inside the interior of the barrel. The nature and size of the amino-acid residues forming the hydrophobic core are conserved in WCI, ETI and STI.

Several β-turns, listed in Table 2, are identified in the WCI structure according to the hydrogen-bonding pattern $O_i \cdots N_{i+3}$ (Venkatachalam, 1968). Some of these turns are found in ETI also. An analysis of the sequences of seven Kunitz (STI) family inhibitors (Shibata *et al.*, 1988) shows that the regions between residues Asp6 and Gly9, Glu13 and Gly16, Asn50 and Ser53, and Asp153 and Gly156 involving β-runs in

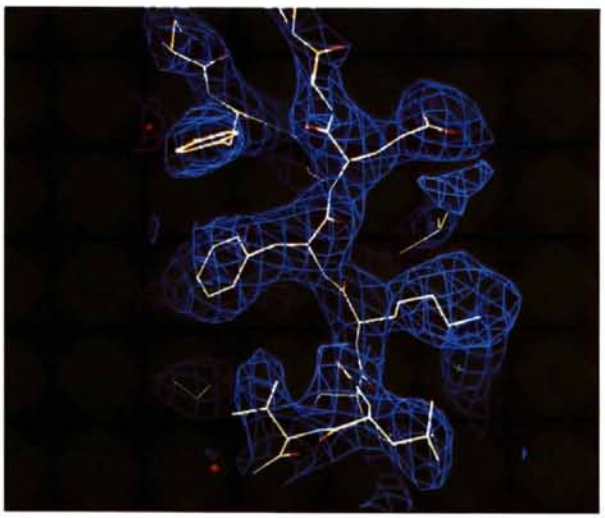

(*a*)

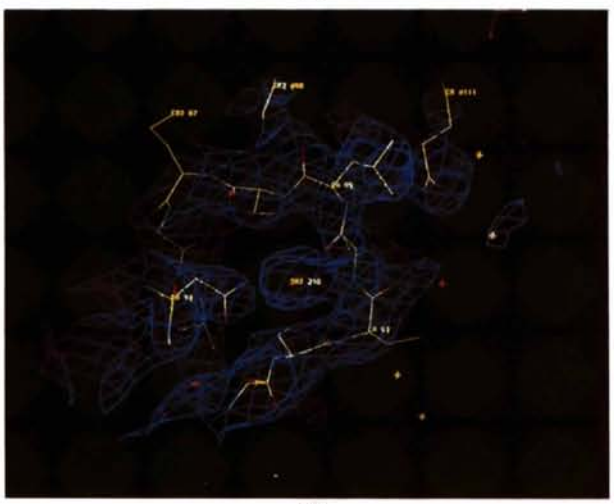

(*b*)

Fig. 1 Representative regions of the $2F_o - F_c$ electron-density map contoured at 1σ, showing: (*a*) part of β-strand 8. (*b*) The reactive-site loop, with the intruding side chain of Asn14 and the water molecule in between.

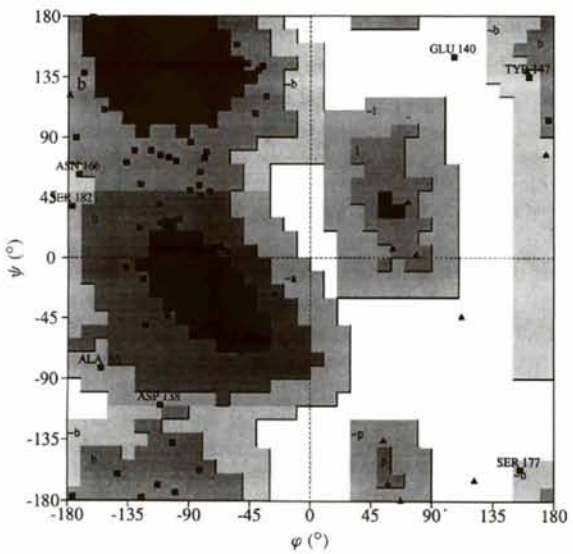

Fig. 2. Ramachandran plot for the WCI structure. Glycine residues are shown as triangles, all others as squares. The regions are marked according to *PROCHECK* (Laskowski *et al.*, 1993).

WCI and ETI, are conserved and presumably have the same secondary structure. The first two turns in the present structure, *viz* Asp6–Gly9 and Glu13–Gly16, bring Asn14 near the reactive-site loop and its side chain intrudes inside the loop cavity. The region between residues Pro110 and Leu115 has both $O_i \cdots N_{i+3}$ and $O_i \cdots N_{i+4}$ types of hydrogen bonding and can be said to have an approximate α-helical conformation as the main-chain dihedral angles of two residues, Pro110 and Glu111, conform to values required to form such a helix.

Altogether four β-bulges can be identified in the structure (one of them is classic and the others G1) according to the hydrogen bonding and the values of dihedral angles prescribed by Richardson (1981). The location and classification of these bulges along with the dihedral angles are given in Table 3.

Table 2. *β-turns in WCI*

Residue Nos.	Amino-acid residues	Type*	φ_2	ψ_2	φ_3	ψ_3
6–9	DAEG	I	−77.9	−30.0	−97.6	28.1
13–16	ENGG	II	−79.9	111.1	72.3	41.1
50–53	NEVS	I	−45.5	−54.5	−82.6	53.7
70–73	PRGS	II	−51.5	144.9	112.0	−44.2
79–82†	PANP		−57.5	−18.0	−130.5	80.0
96–99	SPQG	I	−89.6	−50.2	−60.2	−36.9
110–113	PAVK	I	−58.6	−49.3	−61.2	4.9
153–156	DRNG	I	−59.9	−9.1	−111.3	25.6

* Type classification is according to Venkatachalam (1968). † These four residues form a tight turn. However, the fourth residue being Pro (an imino acid) cannot form a hydrogen bond with the first residue.

3.3. *Conformation of the reactive-site loop*

The general conformation of the reactive-site loop of WCI is similar to that in ETI and STI (Table 4). The side chain of an asparagine residue near the N terminus (Asn14 in WCI) intrudes inside this loop region and forms strong hydrogen bonds with many side-chain and main-chain atoms (Fig. 6). This network of hydrogen bonds stabilizes the loop. Furthermore, the main-chain N atoms of Asn14, Leu4 and Ser73 form hydrogen bonds with carbonyl O atoms of Leu67, Ile69 and Pro70, respectively. Residues Pro70 to Ser73 form a β-turn. The main-chain N atom and the guanidium group of Arg71 and OG of Ser66 are hydrogen bonded to the main-chain carbonyl O atoms of Asp2, Asp1 and Phe68, respectively. The hydrogen-bonding network in WCI is different in detail from that in ETI. IN WCI,)D1 and ND2 of Asn14 are hydrogen bonded to the peptide N atom of Ser62 and the peptide carbonyl O atom of Ser66, respectively, whereas in ETI the corresponding ND2 is hydrogen-bonded to OG of P_4Ser and carbonyl O atom of P_2Ser (following the nomenclature of Schechter & Berger, 1967). In WCI, due to rotation of the $C_\beta—C_\gamma$ bond of Ser62(P_4), its OG is placed away from the ND2 of Asn14 and makes a hydrogen bond with the main-chain N atom of Phe64(P_2). The orientation of the main-chain carbonyl O atom of Leu65(P_1) is such that it is inaccessible to ND2 of Asn14. However, a water molecule, which resides inside the reactive-site loop of WCI, forms hydrogen bonds with the carbonyl O atoms of Phe64 and Ser62 (Fig. 6), and helps to maintain the structure of the loop. This water molecule has not been observed in other inhibitor structures of the Kunitz (STI) family.

As mentioned earlier, WCI is likely to have a second reactive site. Although it has not been possible to unambiguously locate this site, a careful examination of the protein surface appears to suggest

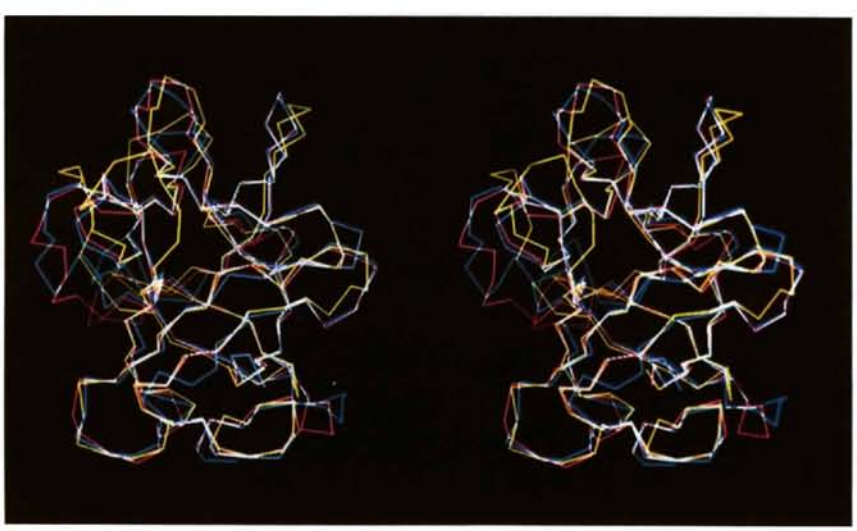

Fig. 3. Superposition of C^α backbones of WCI (red), ETI (cyan) and STI (magenta).

Table 3. *β-bulges in WCI*

The conformational angles ψ and φ are given in parentheses (°) for each residue. Type classification is according to Richardson (1981).

Residue 1	Residue 2	Residue *x*	Type
Gly9 (61.1, 6.7)	Asn10 (−85.6, 164.9)	Asp6 (−82.4, −157.9)	G1
Gly29 (174.1, 76.5)	Gly30 (160.0, 138.5)	Ser48 (−32.9, 120.5)	Classic
Gly15 (72.3, 41.1)	Gly16 (−103.4, 164.7)	Ile60 (121.0, 100.2)	G1
Gly156 (78.6, 2.1)	Asn157 (−69.5, 138.4)	Asp153 (−113.0, 156.6)	G1

Table 4. *Backbone conformational angles at the active-site of three Kunitz-type inhibitors*

↓ Indicates the scissile bond.

	P_4	P_3	P_2	P_1	↓ P_1'	P_2'	P_3'
STI	−58/127	−40/−39	−65/141	−93/47	−93/123	−165/−178	8/49
ETI	−86/171	−69/−28	−115/149	−63/136	−170/161	−79/−34	−118/178
WCI	−125/−177	−85/−22	−89/174	−114/76	−123/158	−89/−20	−131/158

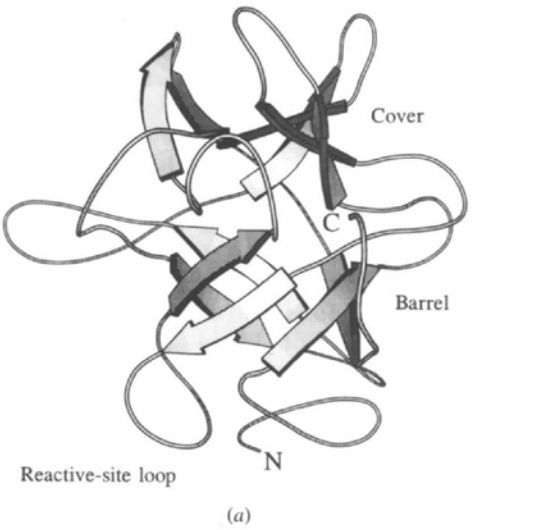

(*a*)

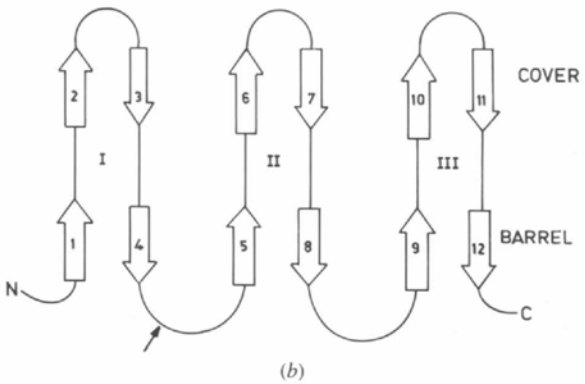

(*b*)

Fig. 4. (*a*) Schematic representation of the conformation of WCI drawn with the program *MOLSCRIPT* (Kraulis, 1991). Arrows represent β-strands. The six-stranded β-barrel is made up of the β-strands 1, 4, 5, 8, 9 and 12 (see *b*). The barrel axis is vertical. The other six β-strands, forming a kind of cover to one open end of the β-barrel, is on the opposite side of the reactive-site loop. (*b*) The secondary structure of WCI. The reactive site is indicated by an arrow.

that it might be on the opposite side of the already indentified reactive site.

3.4. *Intermolecular contacts*

The WCI molecule, in the general position of the space group $P6_122$, makes intermolecular contacts of less than 4 Å with five symmetry-related molecules. Hydrophobic contacts are made by the side chains of residues Leu65 and Leu67 with Pro89* and Trp90* (* represents the symmetry $x-y, -y, -z$). The main-chain carbonyl O atom of Leu65 is hydrogen bonded to NE1 of Trp90*. The residue Leu65 also makes contacts with the residues Glu111* and Ilu114*. Extensive interactions are also made by the side chains of the residues in the exposed loop region such as His23, Ile24 and Trp25 with neighbouring molecules. Trp25, which makes the maximum number of intermolecular contacts, is packed between two symmetry-related molecules (Fig. 7).

The C-terminus residue His183 is hydrogen bonded to the main-chain carbonyl O atom of Pro40*. These two residues are also bridged by a water molecule. There are in all ten intermolecular water bridges in the structure.

This work is supported by a grant (BT/R&D/15/15/92) from the Department of Biotechnology, Government of India. The intensity data were collected at the National facility at IISc, Bangalore, India. The authors also acknowledge the help of Professor T. L. Blundell, Professor D. M. Blow and their colleagues for extending the computational facilities of their laboratories at Birkbeck and Imperial Colleges, London, during a short visit by one of them (AP) at the early stage of the work. Thanks are due to the Computer Centre at

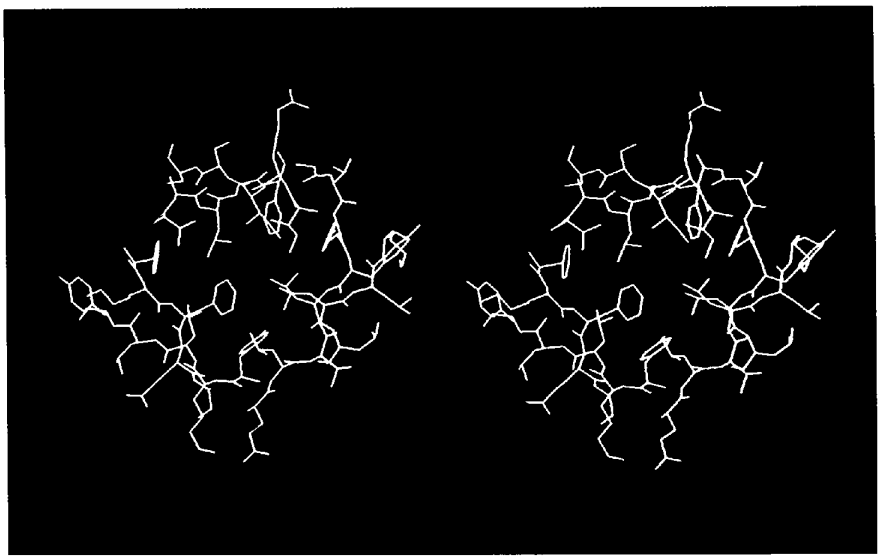

Fig. 5. The hydrophobic core of the β-barrel seen down the barrel axis.

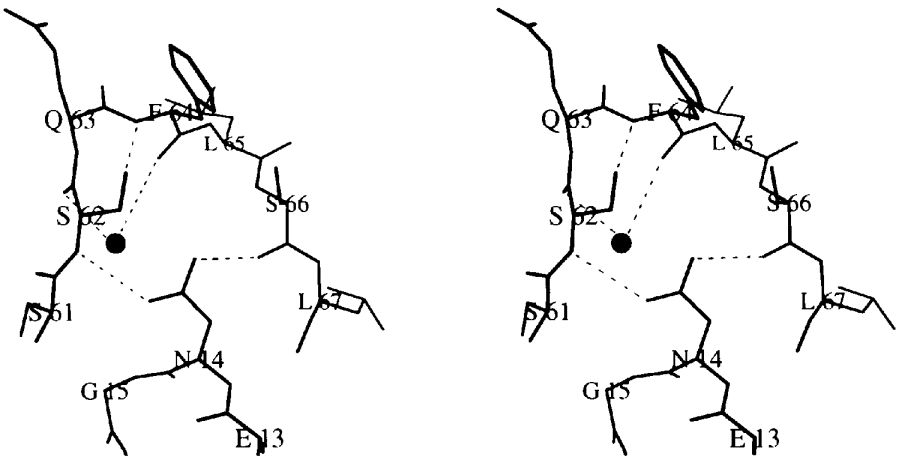

Fig. 6. Hydrogen bonding (indicated by broken lines) in the reactive-site loop. A water O atom is indicated by a dark circle.

the Indian Statistical Institute, Calcutta, India, for help and cooperation.*

* Atomic coordinates and structure factors have been deposited with the Protein Data Bank, Brookhaven National Laboratory (Reference: 1WBC, R1WBCSF). Free copies may be obtained through The Managing Editor, International Union of Crystallography, 5 Abbey Square, Chester CH1 2HU, England (Reference: VJ0004).

References

Blow, D. M., Janin, J. & Sweet, R. M. (1974). *Nature (London)*, **249**, 54–57.

Bode, W. & Huber, R. (1992). *Eur. J. Biochem.* **204**, 433–451.

Brünger, A. T. (1992). *X-PLOR Manual. Version 3.1.* Yale University, New Haven, CT, USA.

Cambillau, C. & Horjales, E. (1987). *J. Mol. Graphics*, **5**, 175–177.

Chothia, C. & Janin, J. (1982). *Biochemistry*, **21**, 3955–3965.

Collaborative Computational Project, Number 4 (1994). *Acta Cryst.* D**50**, 760–763.

Crowther, R. A. (1972). *The Molecular Replacement Method*, edited by M. G. Rossmann, pp. 173–178. New York: Gordon & Breach.

Crowther, R. A. & Blow, D. M. (1967). *Acta Cryst.* **23**, 544–548.

Dattagupta, J. K., Podder, A., Chakrabarti, C., Dutta, S. K. & Singh, M. (1990). *J. Mol. Biol.* **216**, 229–231.

Driessen, H., Haneef, M. I. J., Harris, G. W., Howlin, B., Khan, G., Laskowski, R., Sali, A. & Moss, D. S. (1990). *RESTRAIN V3.13*, Laboratory of Molecular Biology, Department of Crystallography, Birkbeck College, England.

Farber, G. K. & Petsko, G. A. (1990). *Trends Biochem. Sci.* **15**, 229–234.

Finzel, B. C., Clancy, L. L., Holland, D. R., Muchmore, S. W., Watenpaugh, K. D. & Einspahr, H.M. (1989). *J. Mol. Biol.* **209**, 779–791.

Graves, B. J., Hatada, M. H., Hendrickson, W. A., Miller, J. K., Madison, V. S. & Satow, Y. (1990). *Biochemistry,* **29**, 2679–2684.
Howard, A. J., Gilliand, G. L., Finzel, B. C., Poulos, T. L., Ohlendorf, D. H. & Salemme, F. R. (1987). *J. Appl. Cryst.* **20**, 383–387.
Jones, T. A. (1978). *J. Appl. Cryst.* **11**, 262–272.
Kortt, A. A. (1980). *Biochim. Biophys. Acta,* **624**, 237–248.
Kraulis, P. J. (1991). *J. Appl. Cryst.* **24**, 946–950.
Kunitz, M. (1947*a*). *J. Gen. Physiol.* **30**, 291–310.
Kunitz, M. (1947*b*). *J. Gen. Physiol.* **30**, 311–320.
Laemmli, U. K. (1970). *Nature (London),* **227**, 680–685.
Laskowski, M. Jr & Kato, I. (1980). *Annu. Rev. Biochem.,* **49**, 593–626.
Laskowski, R. A., MacArthur, M. W., Moss, D. S. & Thornton, J. M. (1993). *J. Appl. Cryst.* **26**, 283–291.

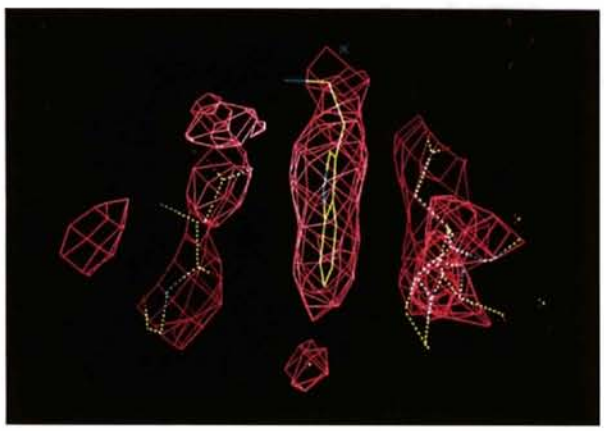

Fig. 7. The electron density in the intermolecular contact region between Trp25 and two symmetry-related molecules.

Laskowski, M. Jr & Sealock, R. W. (1971). *The Enzymes*, **3**, 375–473.
McLachlan, A. D. (1979). *J. Mol. Biol.* **133**, 557–563.
Matthews, B. W. (1968). *J. Mol. Biol.* **33**, 491–497.
Onesti, S., Brick, P. & Blow, D. M. (1991). *J. Mol. Biol.* **217**, 153–176.
Priestle, J. P., Schär, H.-P. & Grütter, M.G. (1988). *EMBO J.* **7**, 339–343.
Priestle, J. P., Schär, H.-P. & Grütter, M. G. (1989). *Proc. Natl Acad. Sci. USA,* **86**, 9667–9671.
Ramakrishnan, C. & Ramachandran, G.N. (1965). *Biophys. J.* **5**, 909–933.
Read, R. J. (1986). *Acta Cryst.* A**42**. 140–149.
Richardson, J. S. (1981). *Advan. Protein Chem.* **34**, 167–363.
Richardson, M. (1977). *Phytochem.* **16**, 159–169.
Roy, A. & Singh, M. (1986). *Phytochem.* **25**, 595–600.
Roy, A. & Singh, M. (1988). *Phytochem.* **27**, 31–34.
Ryan, C. A. (1973). *Annu. Rev. Plant Physiol.* **24**, 173–196.
Ryan, C. A. (1990). *Annu. Rev. Phytopathol.* **28**, 425–449.
Schechter, I. & Berger, A. (1967). *Biochem. Biophys. Res. Commun.* **27**, 157–162.
Shibata, H., Hara, S. & Ikenaka, T. (1988). *J. Biochem. (Tokyo),* **104**, 537–543.
Shibata, H., Hara, S., Ikenaka, T. & Abe, J. (1986). *J. Biochem. (Tokyo)*, **99**, 1147–1155.
Subbarao, N. & Haneef, I. (1991). *Protein Eng.* **4**, 877–884.
Sweet, R. M., Wright, H. T., Janin, J., Chothia, C. H. & Blow, D. M. (1974). *Biochemistry,* **13**, 4212–4228.
Ten Eyck, L. F. (1973). *Acta Cryst.* A**29**, 183–191.
Towbin, H., Staehelin, T. & Gordon, J. (1979). *Proc. Natl Acad. Sci. USA,* **76**, 4350–4354.
Usha, R. & Singh, M. (1995). Unpublished results.
Venkatachalam, C. M. (1968). *Biopolymers,* **6**, 1425–1436.
Zemke, K. J., Müller-Fahrnow, A. Jany, K.-D., Pal, G. P. & Saenger, W. (1991). *FEBS Lett.* **279**, 240–242.